

11-1-2012

Performance of a Beam-Steering Antenna in Interference-limited Multiuser Networks

Z. Li

E. Ahmed

C. P. Sukumar

A. Eltawil

Bedri A. Cetiner
Utah State University

Recommended Citation

Li, Z.; Ahmed, E.; Sukumar, C. P.; Eltawil, A.; and Cetiner, Bedri A., "Performance of a Beam-Steering Antenna in Interference-limited Multiuser Networks" (2012). *ECE Faculty Publications*. Paper 67.
http://digitalcommons.usu.edu/ece_facpub/67

This Article is brought to you for free and open access by the Electrical and Computer Engineering, Department of at DigitalCommons@USU. It has been accepted for inclusion in ECE Faculty Publications by an authorized administrator of DigitalCommons@USU. For more information, please contact becky.thoms@usu.edu.



Performance of a Beam-Steering Antenna in Interference-limited Multiuser Networks

Journal:	<i>IET Microwaves, Antennas & Propagation</i>
Manuscript ID:	MAP-2012-0664
Manuscript Type:	Research Paper
Date Submitted by the Author:	15-Nov-2012
Complete List of Authors:	EITawil, Ahmed; University of California, Irvine, Electrical Engineering Cetiner, Bedri; Utah State University, ECE
Keyword:	ANTENNA ARRAYS, ANTENNA RADIATION PATTERNS, SIGNAL PROCESSING, MOBILE COMMUNICATION, MULTIUSER CHANNELS

SCHOLARONE™
Manuscripts

Performance of a Beam-Steering Antenna in Interference-limited Multiuser Networks

Z.Y. Li, *Student Member, IEEE*, E. Ahmed, *Student Member, IEEE*, C. P. Sukumar, *Member, IEEE*,

A. M. Eltawil, *Member, IEEE*, and B. A. Cetiner, *Member, IEEE*

Abstract—This paper studies the performance gains obtained by utilizing a parasitic layer based beam steering patch antenna in interference limited multiuser networks. The beam-steering antenna employed is capable of steering its beam in three directions ($\theta_m = -30^\circ, 0^\circ, 30^\circ$), where $\theta_m = 0^\circ$ being the broadside direction. The operation frequency range is 5.4 – 5.6 GHz. In the simulations, a directional cluster based channel model is used. Two different beam selection schemes are considered, namely a) Signal to Interference plus Noise Ratio (SINR) and b) Signal to Leakage plus Noise Ratio (SLNR) and the corresponding results have been compared. The results show that this beam steering antenna outperforms the regular patch antennas across all values of SNR with SLNR being a more practical scheme as compared to SINR.

Index Terms—Multifunctional Reconfigurable Antenna, Beam-steering antenna, Multiuser Networks, Interference, Symbol Error Rate

I. INTRODUCTION

In meeting the desired performance characteristics, i.e., high data rate and capacity of wireless networks without compromising the size and cost of the system, multifunctional reconfigurable antennas (MRAs) have gained significant interest during the last several years [1-3]. Specifically in [4] MRAs with reconfigurable polarizations were shown to exhibit superior performance gains. In [5] the capacity of a beam tilting antenna was simulated using ray tracing experiments and was shown to be higher than omnidirectional antennas. MRAs with pattern reconfigurability were also analyzed in [6]. In [7] an analytical study was reported which described the gains and constraints of generic MRA systems. In [8] a comprehensive analysis of capacity and Symbol Error Rates (SER) using a generic channel model was presented. It was shown that single MRA elements could replace multiple omni-directional antennas and maintains either same or superior performance. Also in [9], techniques to

improve system performance by reducing the training overhead for MRAs were presented and characterized.

While most of the contributions so far have assumed MRAs in single user networks, MRAs can also be significantly beneficial in multi user networks. In this paper, we study interference-limited multi user networks. In such systems, Multi-User Interference (MUI) is a major performance limiting factor affecting cell capacity and spectrum efficiency. The results obtained in this work show that significant reduction in the average Symbol Error Rate (SER) can be achieved at the Base Stations (BS) by utilizing beam-steering antennas at each mobile transmitter. Improvement in performance is achieved by picking the beam direction which maximizes the Signal to Interference plus Noise (SINR) ratio of the system. However, this metric requires knowledge of the channels between all transmitter-BS pairs and also involves a large search space. Therefore, a second metric which requires considerably less channel knowledge – the Signal to Leakage plus Noise Ratio (SLNR) [10] is also studied. The contributions of this paper are listed as follows:

1. A new beam-steering patch antenna based on a reconfigurable parasitic layer, which will henceforth be referred to the multifunctional reconfigurable antenna (MRA), has been designed, fabricated and characterized. The radiation patterns obtained by Electro-Magnetic (EM) full wave analysis and by measurements from prototype antennas are used to show practical improvements in SER performance over legacy systems with fixed radiation patterns.
2. An optimum mode selection algorithm based on SINR is utilized. To further reduce the system complexity, the sub-optimal SLNR metric is used and shown not to significantly degrade performance.

II. THE ANTENNA STRUCTURE AND WORKING MECHANISM

The 3-D schematic and cross section view of the beam-steering MRA are depicted in Fig. 1. This MRA uses an air substrate for the parasitic layer and aperture-coupled feed mechanism to achieve improved performance as compared to the MRA presented in [11]. The two main components of the MRA architecture are, namely, the driven patch antenna and parasitic layer. The driven patch ($18 \times 13 \text{ mm}^2$) is designed to operate at $\sim 5.4 \text{ GHz}$ and fed by a $50\text{-}\Omega$ microstrip line through an aperture ($7 \times 0.7 \text{ mm}^2$) etched on the center of the common ground plane as shown in Fig.1. The feed layer ($60 \times 60 \times 0.508 \text{ mm}^3$) and the patch layer ($60 \times 60 \times 1.524 \text{ mm}^3$) are built respectively by using RO4003C ($\epsilon_r = 3.55$, $\tan \delta = 0.002$)

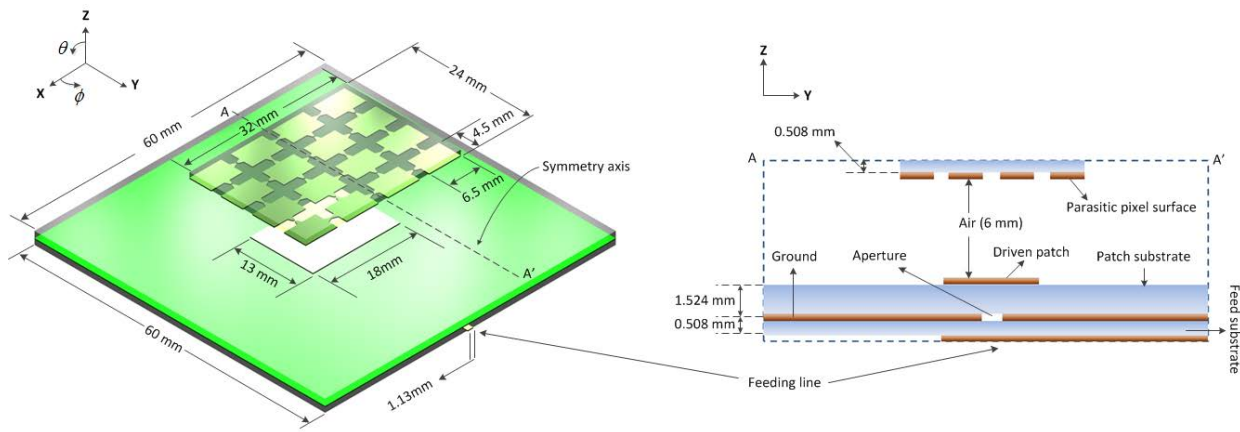


Fig. 1. 3-D Schematic and cross section view of the beam-steering MRA

substrate. The same substrate ($32 \times 24 \times 0.508 \text{ mm}^3$) is also used to form the parasitic pixel surface, which consists of 4×4 rectangular-shaped metallic pixels with individual pixel size being $6.5 \times 4.5 \text{ mm}^2$. The electrical properties of the parasitic layer are determined by a 6mm thick air layer (polymethacrylimide foam with $\epsilon_r = 1.043$), where the main role of the RO4003C substrate is to provide mechanical support for the pixels. The geometry of this parasitic pixel surface can be changed by turning ON or OFF the switches between adjacent pixels, which in turn changes the current distribution of the antenna, resulting in three different beam directions, ($\theta_m = -30^\circ, 0^\circ, 30^\circ$). Full-wave analysis by HFSS [13] and multi-objective genetic algorithm optimization are jointly employed to determine the interconnecting switches' status (i.e., short or open circuit) corresponding to the three modes of operation. Given the symmetric feature of the parasitic layer (see Fig. 1) once the configuration with steering angle θ has been obtained, the corresponding configuration of $(-\theta)$ can be found by mirroring the switch status along the symmetry axis shown in Fig. 1. Notice that in this work, for simplicity, the interconnecting switches between adjacent pixels are replaced by perfect short circuit (ON) or perfect open circuit (OFF).

To validate the theoretical analysis of the beam-steering MRA, three prototypes each of which corresponds to one of the beam steering angle ($\theta_m = -30^\circ, 0^\circ, 30^\circ$) have been designed and fabricated. The measured and simulated reflection coefficients corresponding to the beam-steering modes of $\theta=30^\circ$ and $\theta=0^\circ$ are shown in Fig. 2. The reflection coefficient is only shown for one of the two symmetric beam-steering angles ($\theta=30^\circ$) as the results for $\theta=-30^\circ$ is identical due to the symmetry feature of the parasitic pixel surface. As shown in Fig. 2, the simulated and measured results agree reasonably well, having a 150 MHz common BW around 5.5 GHz as highlighted in this figure. Fig. 3 (a) and 3 (b) show the radiation patterns at the resonant frequency of interest ($\sim 5.5 \text{ GHz}$) of all beam-steering prototypes ($\theta=30^\circ, \theta=-30^\circ, \theta=0^\circ$), respectively. The simulated and measured results agree well indicating that the realized gain values are $\sim 9\text{dB}$ for all beam-steering angles.

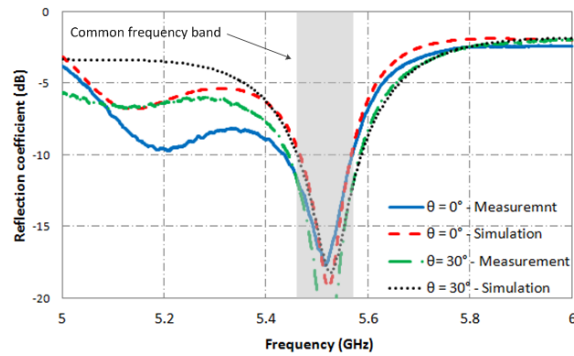


Fig. 2. Measured and simulated reflection coefficients of the MRA prototypes for beam steering angles $\theta = 30^\circ$ and $\theta = 0^\circ$

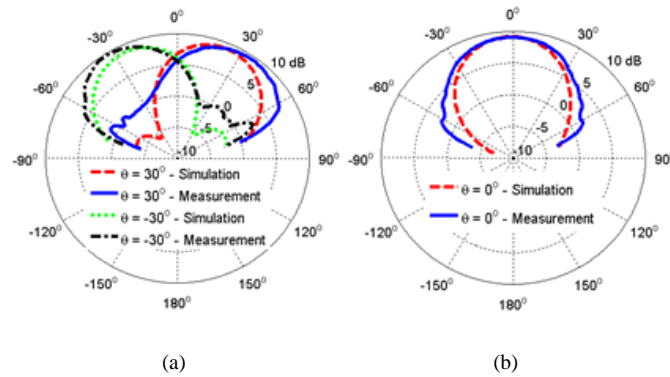


Fig. 3. Measured and simulated realized gain patterns of the beam-steering MRA prototypes for (a) $\theta = 30^\circ$ and $\theta = -30^\circ$ and (b) $\theta = 0^\circ$. The patterns are cut in the x-z plane at the center frequency, 5.5 GHz

III. SYSTEM MODEL

The network geometry is as follows. We consider a scenario with R multiple transmitter-BS uplink pairs that access the wireless medium at the same frequency band. Throughout this paper we assume that the number of antennas at both the transmitters and BS is one. The BS receivers are assumed to be equipped with regular omni-directional antenna while for the Mobile Station (MS) two scenarios are considered a) MS transmitters are equipped with regular patch antennas, b) MS transmitters are equipped with a beam-steering MRA introduced in section II.

Each channel is modeled using cluster based channel modeling [15]-[17]. The clusters are assumed to be uniformly distributed between 0 and 2π around the BS. Each MRA is capable of pointing in one of $N_{dir}=3$, ($\theta_m = -30^\circ, 0^\circ, 30^\circ$), beam directions. The channel in the j^{th} direction from the p^{th} multipath between the x^{th} transmitter and y^{th} BS can be written as follows [6]:

$$h^{(j)}_p \{x \rightarrow y\} = \sqrt{\alpha \{x \rightarrow y\}} \left\{ \sqrt{\frac{K_p}{K_p + 1}} h_{\text{fixed}} \{x \rightarrow y\} \sqrt{G^{(j)}(\theta_{\text{LoS}})} + \sqrt{\frac{1}{K_p + 1}} \sum_{c=1}^{N_{cl}} (\sqrt{P^{(j)}_{c,p}} \cdot r_{c,p}) \right\} \quad 1$$

where $\alpha \{x \rightarrow y\}$ is the power coefficient explained below, K_p is the Ricean factor for the p^{th} multipath, $h_{\text{fixed}} \{x \rightarrow y\}$ is the Line of Sight (LoS) coefficient, G represents the radiation pattern, θ_{LoS} is the LoS angle, N_{cl} is the number of clusters in the RF environment, $P^{(j)}_{c,p}$ is the power received from the c^{th} cluster and the p^{th} multipath in the j^{th} direction and is computed as given in [6] (although the computation is performed for MRAs at the receiver, due to the reciprocal nature of the channel, the same framework can be used). $r_{c,p}$ is the Rayleigh fading non-LOS component. For regular patch antennas, the channel can be generated using the same expression with $G(\theta)$ measured from a regular patch antenna. The direction j however, clearly loses meaning in this case. The power coefficient $\alpha \{x \rightarrow y\}$ is the power attenuation due to path loss between transmitter x and BS y normalized to the path loss between the transmitter and intended BS. Thus, in this paper, $\alpha \{x \rightarrow x\}$ which is the attenuation between the x^{th} transmitter-BS pair is always 1, while $\alpha \{x \rightarrow y\}$ is the attenuation between the x^{th} transmitter and the y^{th} BS pair which contributes to multi user interference.

Another assumption that is made is that the clusters around a particular receiver do not affect the channel between transmitters and other receivers. This assumption is valid because typically the distance between these clusters and other receivers is high and thus the path loss ensures that the signal from these clusters has much less power than other signals.

Orthogonal Frequency Division Multiplexing (OFDM) is chosen as the modulation of choice due to its resilience in frequency selective environments. The number of subcarriers is assumed to be N_{FFT} . To induce cyclic convolution and to protect against Inter-Block Interference (IBI), a cyclic prefix of length N_{cp} is pre-pended to the OFDM symbol. It is assumed that transmitter d communicates with BS d and all other transmitters (1 thru R not including d) contribute to interference. The received signal in the frequency domain at BS d is given by the following expression:

$$Y_{d,k} = H_k^{j_d} \{d \rightarrow d\} X_{d,k} + \sum_{m=1, m \neq d}^R H_k^{j_m} \{m \rightarrow d\} X_{m,k} + n_{d,k} \quad 2$$

where at the k^{th} subcarrier, $H_k^{j_x} \{x \rightarrow y\}$ is the channel in the j_x direction between the x^{th} transmitter and the y^{th} BS, $X_{m,k}$ is the transmitted data from the m^{th} transmitter and $n_{d,k}$ is AWGN with variance σ^2 . The transmit power of the u^{th} transmitter is

given by $P_u = \sum_{k=0}^{N_{\text{FFT}}-1} \|X_{u,k}\|^2$. To reduce SER, each transmitter must pick a direction that maximizes SINR. If transmitter one is

pointing in direction j_1 and transmitter 2 is pointing to direction j_2 and so on, the l^{th} mode is denoted by:

$$\mathbf{j}_l = \{j_1, j_2, \dots, j_R\} \quad 3$$

where $j_i \in \{1, \dots, N_{dir}^R\}$. The maximum number of modes is N_{dir}^R , i.e. $l \in \{1, \dots, N_{dir}^R\}$. SINR for the l^{th} mode at the u^{th} BS and k^{th} subcarrier can be calculated as follows

$$SINR_{u,k}^l = \frac{\left| H_k^{j_u} \{u \rightarrow u\} \right|^2 \cdot \frac{P_u}{N_{FFT}}}{\sigma^2 + \sum_{d=1, d \neq u}^R \left| H_k^{j_d} \{d \rightarrow u\} \right|^2 \cdot \frac{P_d}{N_{FFT}}} \quad 4$$

The numerator represents the power of the desired signal. The denominator is the sum of the channel noise power and the interference from other transmitters at the current receiver. The optimum mode that minimizes SER can be found by performing an exhaustive search across all modes and is concisely represented by equation (5).

$$\mathbf{j}_{opt} = \arg \min_{1 \leq j \leq N_{dir}^R} \sum_{u=1}^R \sum_{k=0}^{N_{FFT}-1} \int_0^{\frac{(M-1)\pi}{M}} \exp \left\{ \frac{-SINR_{u,k}^j \sin^2 \left(\frac{\pi}{M} \right)}{\sin^2 \theta} \right\} d\theta \quad 5$$

where the formula for SER of an M-PSK constellation is used.

Although this is the optimal metric, it has the following disadvantages: a) the channel coefficients between all possible transmitter–BS pairs must be available to all transmitters b) Maximizing the above equation involves searching across N_{dir}^R modes which can reach extremely large values for even small values of R .

To mitigate these disadvantages a second metric Signal to Leakage plus Noise Ratio (SLNR) is chosen. Network SLNR can be maximized by maximizing the SLNR for each user in contrast with SINR. In other words, choosing the optimum direction of a particular transmitter is independent of the direction chosen for other transmitters. The SLNR for a particular user is given by,

$$SLNR_u^j = \sum_{k=0}^{N_{FFT}-1} \frac{\left| H_k^j \{u \rightarrow u\} \right|^2 \cdot \frac{P_u}{N_{FFT}}}{\sigma^2 + \sum_{d=1, d \neq u}^R \left| H_k^j \{u \rightarrow d\} \right|^2 \cdot \frac{P_u}{N_{FFT}}} \quad 6$$

The numerator represents the power of the desired signal at the u^{th} receiver. The denominator is the sum of the channel noise and the interference at other receivers due to the u^{th} transmitter. The optimum direction to maximize SLNR for the u^{th} user is given by:

$$j_{opt}^{(u)} = \arg \max_{1 \leq j \leq N_{dir}^R} SLNR_u^j \quad 7$$

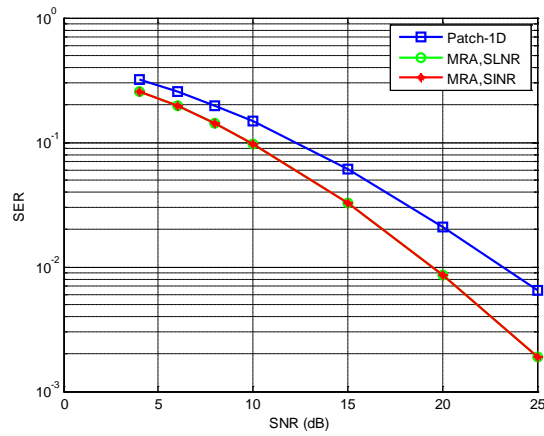
To minimize the average SER throughout the network, the sum of all SLNRs should be maximized by choosing the optimum direction for each user as shown above. This is in contrast with the SINR metric in which a non-linear equation has to be computed across the global network.

IV. SIMULATION RESULTS

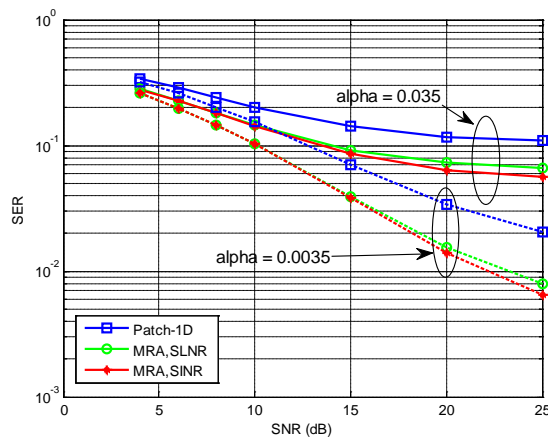
In this section the gains obtained by utilizing the beam-steering MRA (presented in section II) in multi-user networks are detailed. Each subcarrier carries a data symbol modulated using 4-QAM. The number of subcarriers (N_{FFT}) is chosen to be 1024 with the length of cyclic prefix $N_{cp} = 128$. The system bandwidth (BW) is 10MHz. Two channel models are used in simulations [15]-[17] a) Channel model 1 is used as a typical indoor channel model, which has 2 clusters with a maximum delay spread of 80ns, b) channel model 2 is used as a typical outdoor channel model, which has 6 clusters with a maximum delay spread of 1050ns. Four transmit-receive pairs are simulated.

In Fig. 4.a and Fig. 4.b the indoor SER performance of the regular patch antennas and the MRAs presented in section II using SINR and SLNR direction selection schemes are quantified for values of $\alpha = 0, 0.0035, 0.035$ respectively. These values of α are the power attenuation coefficients for only the channels between a transmitter and an unintended receiver (BS). The values of α are equivalent to Infinte, 10 and 20 dB Signal to Interferer ratio (SIR) at each receiver respectively. As mentioned before, $\alpha = 1$ for channels between a transmitter and the intended receiver (BS). A value of $\alpha = 0$ clearly corresponds to a network where there is zero multi-user interference. Regardless of selection scheme and channel model, across all values of α and SNR, MRAs outperform their regular patch counterparts, which have a fixed beam direction along the broadside direction. As mentioned before SINR is the optimum scheme and therefore achieves lower SER than the SLNR scheme. While both schemes require about 10dB less SNR to achieve a SER of 10^{-1} (for the radiation patterns presented here and $\alpha = 0.035$) than regular patch antenna, the difference between SINR and SLNR is less than 1dB. However, the difference between the two schemes increases at higher SNRs. This is because the contribution to SER degradation from interference is more prominent compared to channel noise in that region. This affects SLNR more than SINR due to the increased interference resulting from non-optimum direction selection. Despite the marginal improvement in performance, SLNR is a more practical choice for selection scheme due to the two following reasons: a) for SINR selection the CSI for all existing channels have to be available at each transmitter b) the computation complexity of SINR is prohibitive.

In Fig. 5, the SER performance for outdoor and indoor channels is compared for $\alpha = 0.0035$. The results show that having a beam steering MRA improves system performance in both outdoor and indoor environments. It also shows that increasing the number of clusters degrades the system performance when MRA is used. This is because, increasing the number of clusters around the receiver increases the probability of having an interferer signal reflected from different transmit directions which leads to a lower SINR at the receiver side. On the other hand, increasing the number of clusters improves the performance when a regular patch antenna with a fixed beam direction is used. This is due to the fact that when using a regular patch antenna, a larger number of clusters results in more diversity gains at the receiver side. However, in the case of the MRAs, the directionality gain achieved by the MRA is larger than the diversity gain achieved by the increased number of clusters.



(a)



(b)

Fig. 4. (a) SER vs. SNR, regular patch antenna and MRA with $N_{dir}=3$ and $\alpha=0$, (b) SER vs. SNR, regular patch antenna and MRA with $N_{dir}=3$ and $\alpha=0.035, 0.0035$

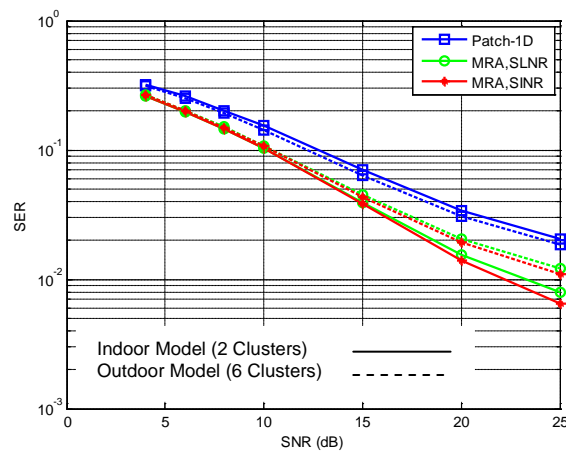


Fig. 5. SER vs. SNR, regular patch antenna and MRA for indoor and outdoor channel models and $\alpha=0.0035$

V. CONCLUSION

In this paper, we propose a novel parasitic layer based beam steering multifunctional reconfigurable antenna (MRA) and study the performance improvements obtained by utilizing such an antenna at the transmitter in interference-limited multi-user networks. This beam-steering MRA, which is based on a reconfigurable parasitic layer, has been designed, fabricated and characterized. The radiation patterns obtained by Electro-Magnetic (EM) full wave analysis and by measurements from prototype antennas were used to demonstrate performance improvements in terms of SER over regular patch antennas. Two beam selection schemes were presented based on SINR and SLNR metrics. It was shown that although SINR achieves slightly lower SER, SLNR was found to achieve comparable performance while being a more practical scheme.

REFERENCES

- [1] J. T. Bernhard, "Reconfigurable Antennas," *Synthesis Lectures on Antennas*, San Rafael, CA: Morgan & Claypool, 2007
- [2] B. A. Cetiner *et al.*, "Multifunctional reconfigurable MEMS integrated antennas for adaptive MIMO systems," *IEEE Commun. Mag.*, vol. 42, pp. 62–70, Dec. 2004.
- [3] B. A. Cetiner, E. Sengul, E. Akay, E. Ayanoglu "A MIMO system with multifunctional reconfigurable antennas" *IEEE Antennas and Wireless Propagation Letters*, Vol. 5, pp. 463-466, December 2006
- [4] J. Boerman and J. T. Bernhard, "Performance study of pattern reconfigurable antennas in MIMO communication systems," *IEEE Trans Antennas Propag.*, vol. 56, no. 1, pp. 231-236, Jan. 2008.
- [5] D. Piazza *et al.*, "Design and evaluation of a reconfigurable antenna array for MIMO systems," *IEEE Trans. Antennas Propag.*, vol 56, no. 3, pp. 869-881, 2008.
- [6] A. Grau, H. Jafarkhani, and Franco De Flaviis, "Reconfigurable MIMO Communication System," *IEEE Trans. Wireless Commun.*, Vol. 7, No. 5, pp. 1719 – 1733, May 2008.
- [7] C. P. Sukumar, H. Elsami, A. Eltawil, and B. A. Cetiner "Link Performance Improvement using Reconfigurable Multi-Antenna Systems," *IEEE Antennas and Wireless Propagation Letters*, Vol. 8, pp: 873 – 876, 2009
- [8] H. Eslami, C. P. Sukumar, D. Rodrigo, S. Mopidevi, A. M. Eltawil, L. Jofre and B. A. Cetiner, "Reduced Overhead Training for Multi Reconfigurable Antennas with Beam-tilting Capability," accepted for publication in *IEEE Transactions on Wireless Communications*.
- [9] D. Gesbert, S. Hanly, H. Huang, S. Shamaï Shitz, O. Simeone, and W. Yu, "Multi-Cell MIMO Cooperative Networks: A New Look at Interference," *IEEE Journal On Selected Areas In Communications*, Vol. 28, No. 9, December 2010
- [10] X. Yuan, Z. Li, D. Rodrigo, H. S. Mopidevi, O. Kaynar, L. Jofre and B. A. Cetiner, "A Parasitic Layer-Based Reconfigurable Antenna Design by Multi-Objective Optimization," *IEEE Trans. Antennas Propag.*, vol. 60, no. 6, pp. 2690–2701, Jun. 2012
- [11] ANSOFT HFSS, Version 11.0, Build: July 18 2007, ANSYS Corporation, <http://www.ansys.com>
- [12] Sadek, M.; Tarighat, A.; Sayed, A.H., "A Leakage-Based Precoding Scheme for Downlink Multi-User MIMO Channels," *Wireless Communications, IEEE Transactions on*, vol.6, no.5, pp.1711-1721, May 2007 (11)
- [13] A. A. Saleh and R. A. Valenzuela "A Statistical Model for Indoor Multipath Propagation," *IEEE Journal on Selected Areas in Communication*, vol. SAC-5, no. 2, pp. 128-137, Feb. 1987. (12)

- [14] K. Pedersen, *et. al.*, "A stochastic model of the temporal and azimuthal dispersion seen at the base station in outdoor propagation environments" *IEEE Trans. Veh. Technol.*, vol. 49, pp. 437-447, Mar. 2000 (13)
- [15] V. Erceg, L. Schumacher, et al. "TGn channel models," IEEE 802.11-03/940r4, May 2004.